

DeForest Mellon Jr., Matthew A. Reidenbach

Contents

Abstract	159	5. Adaptations to terrestrial lifestyle	167
1. Introduction	159	Conclusions	169
2. Aesthetasc distribution and flicking	160	Acknowledgments	169
3. Fluid mechanical consequences of flicking	161	References	169
4. Comparative aspects	163		

Abstract

Aquatic crustaceans detect odorants in their fluid environment using batteries of microscopic cuticular sensilla, termed aesthetascs, which are arrayed along their antennules. Because these structures are tiny they operate at small Reynolds numbers, implying that fluid flow around and within the sensor arrays is laminar. Access of odorants to the surface of the aesthetascs therefore occurs primarily via molecular diffusion, a process that in most crustacean species appears to be enhanced by antennular flicking behavior. Depending upon the density of the sensor array and the size and structure of the individual aesthetascs, flicking may enhance 'leakiness' of the flow through the sensor array, thereby decreasing the distance over which odorant-laden fluid must be molecularly diffused to the surface of the individual aesthetascs. Here we review theoretical considerations of the fluid mechanics involved with

odorant access to olfactory sensors on the antennules of aquatic crustaceans, including the nature of some remaining unanswered questions, and a brief comparison with the situation in crustaceans that exhibit a terrestrial lifestyle.

1. Introduction

Crustaceans have a central nervous system largely devoted to capturing and analyzing the olfactory environment. Much of their brain (as much as 40 % in some species, but 50 % or more in terrestrial hermit crabs) is devoted to the analysis of incoming olfactory signals, integrating those signals with inputs from visual, mechanical and taste receptors on the head appendages, and to generating behaviors that enhance their efficiency in detecting olfactory signals. There are significant gaps in our understanding of these processes at the cellular and sub-cellular level. For example, crustaceans have

DeForest Mellon Jr.
University of Virginia, Department of Biology
Gilmer Hall, McCormick Road
Charlottesville, VA 22901, USA
e-mail: dm6d@cms.mail.virginia.edu

contact chemoreceptors on their legs as well as on their antennae. A major aspect of active chemoreception in crustaceans involves probing the substrate with their dactyls, probably integrating the chemosensory input with the simultaneous input from contact mechanoreceptor neurons housed within the same sensilla. We have little understanding of how this integration between this particular subset of chemical sensors and mechanoreceptors occurs and how it is used to aid in detecting and processing odorant signals. We also have little understanding of how information obtained from contact chemoreceptor sensilla located on their dactyls integrates with that from the olfactory sensilla located on their antennules. A separate but related problem is how crustaceans utilize multiple signals obtained from the environment to track an odorant to its source by locomotion upstream. Water or air-borne odorants are detected with the aid of their antennules and in almost all crustacean species, these animals are capable of flicking their antennules. This chapter will focus on remaining problems pertaining to the fluid mechanical aspects of this phenomenon.

The antennules of aquatic and terrestrial crustaceans are their nose and are equipped with batteries of odorant-detecting sensilla. The sensilla are microscopic structures that operate at small Reynolds numbers. The Reynolds number, Re , is a measure of the ratio of inertial to viscous forces; it is calculated from the formula $Re = UL/\nu$, where U is velocity, L is diameter of the object being considered, and ν is the kinematic viscosity. For large Reynolds numbers ($\gg 1$), fluid flow is turbulent and the distribution of odorants is controlled by turbulent mixing processes, while for small Reynolds numbers the flow is laminar and odorant distributions are controlled by molecular diffusion. Therefore, even though the distribution of odorants within ambient flows in oceans, streams, and

the atmosphere is typically turbulent, transport on the small scale to the surfaces of chemosensory sensilla occurs under laminar conditions where slow molecular diffusion dominates. How does antennular flicking enhance odorant capture in this laminar flow environment? We herewith review what is currently understood, and what remains to be explained, about the fluid mechanics of crustacean antennular flicking.

2. **Aesthetasc distribution and flicking**

Odorants are scalar quantities imbedded in fluid environments. They are distributed from their sources by large-scale advective, turbulent flow as patchy filaments that vary in space, time, and density relative to the odorant source (Fig. 1). These filamentous odorant signals are sampled by the olfactory organs of the animals and may provide information about the location of the odorant source (Finelli et al. 1999; Webster et al. 2001; Grasso and Basil 2002). Microscale access of odorants to olfactory receptors in general, and to those of aquatic crustaceans in particular, is characterized by laminar flow within arrays of small specialized sensilla situated on the antennules (first antennae). These sensilla, referred to as aesthetascs in crustaceans, are blunt-tipped setae 100–1700 μm long by 10–30 μm in diameter, depending upon the species (Snow 1973; Tierney et al. 1986; Mellon et al. 1989) and occur in arrays on the ventral surface of the more lateral of two mobile flagella on each antennule (Fig. 2).

In almost all crustacean species the aesthetasc-bearing flagellum is capable of flicking behavior, by which the flagellar shaft is quickly moved directly or obliquely ventrally

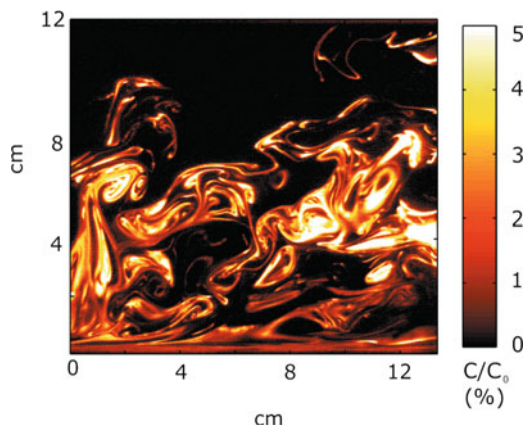


Fig. 1 Planar laser induced fluorescence image of odorant distribution 1.5 m downstream from where the source odorant was released into the flow. A 488 nm wavelength laser illuminated fluorescein dye embedded within the odorant release. Flow was created within a 25 m long laboratory flume with a mean water velocity of 7 cm/s, with movement from left to right in the image, within a total water depth of 25 cm. Concentration, C , is normalized by the percent of the source concentration, C_0 .

for a short distance and then is returned to its previous, normal posture.

Antennular flicking has attracted attention due to its obvious association with olfactory reception. This flicking is analogous to taking a “sniff” of odorant. However, the purpose of flicking has not always been met with universal agreement. This may in part be the result of anatomical differences among crustacean species with respect to the dimensions of the individual aesthetascs and, especially, with the pattern and density of their arrays on the antennular flagella. In hermit crabs and true crabs, (for example, the blue crab *Callinectes sapidus*) the aesthetascs are grouped in a high-density tuft near the tip of their lateral antennular flagellum (Fig. 2). In spiny lobsters the aesthetasc array is also dense but extends along the ventral surface of the antennule for a longer relative distance, rather than being confined to a short tuft. This lengthwise distri-

bution of a high density array is even more extended in clawed lobsters, such as *Homarus americanus*. At the other end of the density/distribution spectrum, the array of aesthetascs in freshwater crayfish extends along the entire ventral half of the lateral antennular flagellum, and the distribution of aesthetascs along the flagellum varies from a sparse one or two per antennular annulus at the proximal end of the array to no more than four per annulus near the distal end of the array (Fig. 3).

3. Fluid mechanical consequences of flicking

In the hermit crab *Pagurus alaskensis*, the downward flick of the lateral flagellum initiates a dramatic splaying action of the dense aesthetasc tuft (Snow 1973), causing spatial separation of the distal regions of the individual sensilla, that portion of each sensillar shaft believed to be permeable to dissolved odorants (Ghiradella et al. 1968; Tierney et al. 1986). As discussed below, that physical separation and the velocity of the flick initiating the splaying action can play a critical role in the access of odorant-bearing fluid to the surface of an aesthetasc. It is not known whether this sort of splaying action is found in other species beyond crabs; it has not been reported in either spiny or clawed lobsters.

Early analyses of the fluid mechanical effects experienced by flicking antennules were undertaken by Cheer and Koehl (1987a, b). Objects moving within a fluid volume are surrounded by a boundary layer of sheared fluid: the molecular fluid layer next to the moving object is stationary, whereas layers farther out from the object are char-

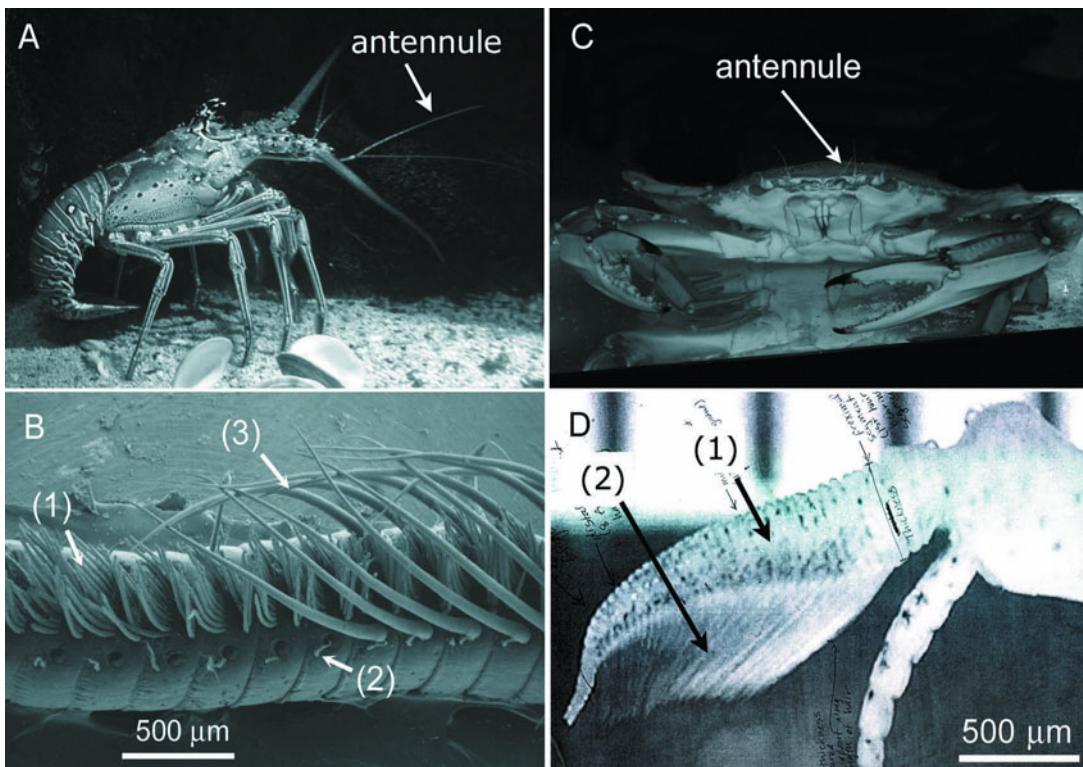


Fig. 2 **A** The spiny lobster, *Panulirus argus*, with lateral antennule labeled. **B** Scanning electron micrograph of the lateral antennule with the (1) chemosensory aesthetascs, (2) mechanosensory sensilla, and (3) guard hairs, labeled. Note that the guard hairs on the left hand side of the image have been removed to expose the aesthetascs (photo courtesy of J. A. Goldman). **C** The blue crab, *Callinectes sapidus*. **D** Antennules of *C. sapidus* with the (1) lateral antennule and (2) chemosensory aesthetascs labeled. *C. sapidus* aesthetascs splay out to increase the distance between the hairs during the flick, and clump back together during the return stroke. (photo courtesy of M. M. Martinez)

acterized by increasing velocity, eventually reaching a value identical with the bulk flow. The thickness and gradient steepness of the sheared layer next to an object depend upon the fluid's viscosity, object's size, and its velocity relative to the fluid. With very small objects, which have a low Reynolds number, or with objects moving slowly through the fluid, the boundary layer is very thick. *Re*'s of most arthropod olfactory receptor sensilla fall within the range of 10^{-4} –10 (Louden et al. 1994). When spacing between individuals of an array of tiny objects, such as aesthetascs, becomes sufficiently small, their boundary layers interfere with each other and the array acts more like a paddle than

like a sieve, preventing fluid from leaking between the aesthetascs. This can present a serious impediment to the free access of odorant molecules to the surface cuticle of the aesthetascs themselves. Within limits, however, this problem may be overcome by increasing the velocity of the aesthetasc array relative to the fluid environment, thereby also decreasing the thickness of the boundary layers (Stacey et al. 2002). It has been argued that antennular flicking has evolved to sub-serve this function. For arrays of sensilla where the spacing between them is less than five times their average diameter, their leakiness is very sensitive to changes in sensillar velocity within the *Re* range of

0.1–10 (Cheer and Koehl 1987a; Koehl 1995, 2000; Koehl et al. 2001; Reidenbach and Koehl 2008). Because the relative velocity of an aesthetasc during an antennular flick depends upon its position upon the flagellar shaft, the extent and placement of the sensillar array can be important. To understand the functional significance of antennular flicking for olfactory reception, therefore, it is critical to know the range of Re values within which the olfactory sensilla operate, realizing that different sizes of individual aesthetascs, their spacing, placement, and the range and velocity of antennular movements play an integrated determinative role in the parameter effectiveness of the different species. The spiny lobster *Panulirus argus*, as mentioned above, possesses an aesthetasc array characterized by close spacing along a restricted region of the more distal antennular shaft. This structure has been the subject of theoretical, modeling, and experimental studies which indicate that given the mechanical properties of the aesthetascs, their position along the flagellum, and the density of their array, the downward flick of the lateral flagellum, occurring at a $Re = 1$ to 2, reduces the boundary layer of fluid around the individual aesthetascs. This allows the array to become sufficiently leaky for fluid exchange to occur during the downward flick phase of the flick-return cycle (Koehl et al. 2001; Reidenbach et al. 2008). These same studies show that, by contrast, during the slower upward return phase, occurring at a $Re = 0.5$, odorant-bearing fluid is trapped within the array, and provides time for molecular diffusion to occur across the cuticle of the individual aesthetascs, increasing the probability of odorant molecules binding with olfactory receptors within the lumen of the individual aesthetascs.

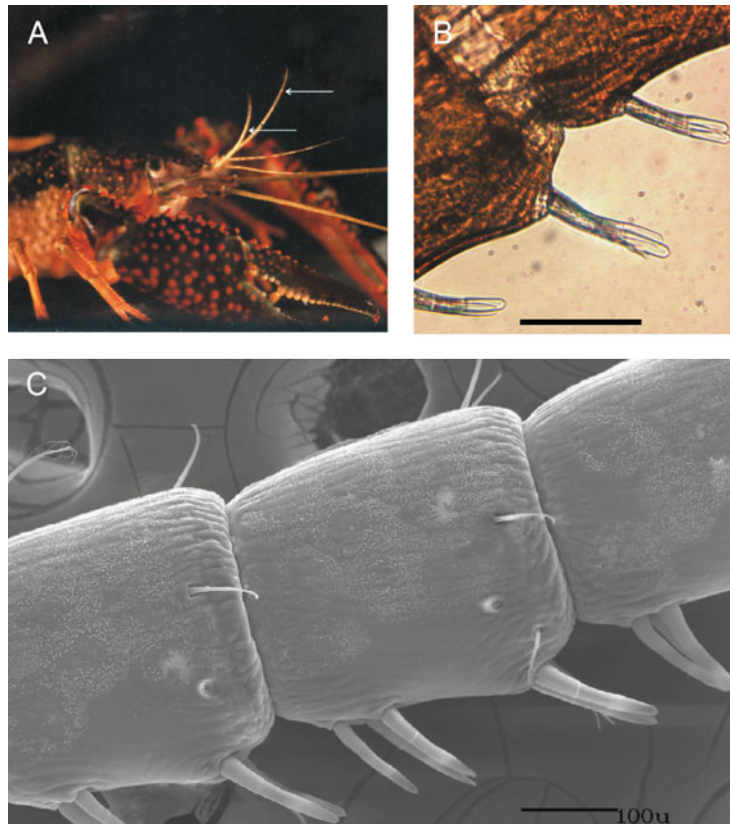
4.

Comparative aspects

From comparable analyses of aesthetasc arrays characterized by very different sizes, morphologies, packing density and spatial distribution characteristics of other species, one can derive hypotheses driven by fluid mechanical considerations. Similar fluid mechanical principles that have provided insight into spiny lobster flicking should be able to be applied within this varied species-dependent context to reveal the functional significance of such diversity for the animals on which they are found. For example, hypotheses could be formed concerning the constraints that have driven the evolution of different aesthetasc densities and distributions. One such crustacean that exhibits very different aesthetasc distribution compared to that of the spiny lobster is the freshwater crayfish *Procambarus clarkii* (Fig. 3). Its aesthetasc-bearing lateral flagella of the antennules are normally held in a curved, partially-vertical orientation (Fig. 3A). The aesthetascs are arrayed ventrally along the distal one-half of each flagellum, emerging from the flagellar surface at an approximately 45° angle (Fig. 3B and C).

Figure 3C shows the distal half of the flagellum, where the aesthetasc array is characterized by pairs of (or occasionally, three) sensilla on each annulus, positioned distally. Each sensillum is approximately 100 μm long and 15–20 μm in diameter at its base, tapering to less than 10 μm at the tip. A clear discontinuity occurs in the aesthetasc structure about three fifths of the way from the base to the tip, where the cuticle becomes optically transparent (Fig. 3B). It is in this region that the aesthetascs are believed also to be transparent to odorant molecules (Ghiradella et al. 1968; Tierney et al. 1986). Therefore, the most important fluid mechanical considerations in odorant capture

Fig. 3 **A** Front view of the crayfish *Procambarus clarkii* indicating the lateral antennular flagella (white arrows) in their usual upright resting posture. **B** Light micrograph of a living lateral flagellum and three pairs of aesthetascs on its ventral surface photographed with bright-field illumination. Note how optically transparent the distal regions are compared to the basal shafts. **C** Scanning electron micrograph of a portion of a fixed lateral flagellum showing the normal placement and spacing of aesthetascs on the flagellar annuli. Scale marks: 100 μm . **A** is reproduced with permission from Mellon and Humphrey (2007)



will be those concerning the tip region of the aesthetasc shaft. It is salient to mention that the individual aesthetascs of a pair are separated at their tip region only by about one diameter, and this has implications for leakiness of the pair to odorant-laden fluid flow.

Individuals of *P. clarkii* flick their antennules spontaneously as well as in response to hydrodynamic and odor stimuli (Mellon 1997). The video frames shown in Fig. 4 are from a series taken during a single flick cycle. Each frame represents 30 msec; Fig. 4A and 4B were taken 180 msec apart during which time the tip of the flagellum was depressed by about 6 mm*. The mean linear velocity of a point on the ventral aspect of the flagellum must therefore have been approximately 0.03 m/sec, and during the downward flick

the Re of an aesthetasc tip region would therefore be

$$Re = (10^{-5} \text{ m} \cdot 0.03 \text{ m/sec}) / 1.00 \cdot 10^{-6} \text{ m}^2/\text{sec} = 0.3$$

Although this value is less than the $Re = 1$ to 2 value calculated for spiny lobster aesthetascs during an average downward flick (Goldman and Koehl 2001), it is well within the range of values in which velocity can make a difference in the leakiness of an array of sensilla. However, as indicated by Fig. 3, side-by-side spacing of the aesthetascs in *P. clarkii* is less than one diameter, similar to the situation in another crayfish, *Orconectes propinquus* (Tierney et al. 1986, cf Fig. 1); thus, crucial questions remain concerning

* At the tip the distance traveled will be less, since the distal part of the flagellum is flexible and lags the main shaft during the initial flick (Fig. 3B).

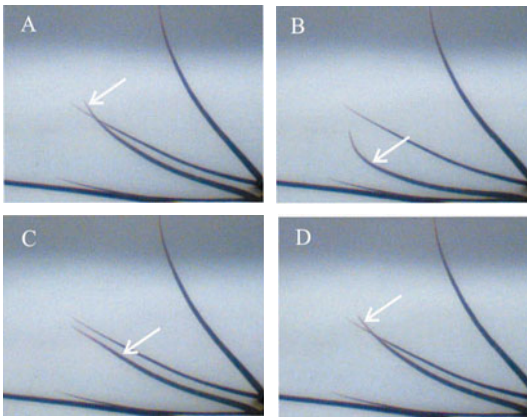


Fig. 4 Video frames from one complete flick sequence. **A** Lateral flagellum (white arrows) posture at rest, prior to downward flick. **B** Flagellum position just prior to termination of downward flick, about 180 msec after frame in **A**. **C** During the recovery phase of the flick; most of the flagellum maintains a rigid form during the upstroke. **D** Frame taken just after the flagellum arrived at the original rest posture

the effects of close inter-aesthetasc spacing and the extent to which they are sufficiently leaky to be maximally exposed to fresh odorant-bearing water during the flick cycle.

Aesthetascs occur along the ventral margin of the lateral antennular flagellum, and it is important to discuss whether fluid mechanical properties of the flagellar shaft itself influence access of odorant-laden water to the sensor array. Humphrey and Mellon (2007) mathematically modeled the flow field past the lateral flagellum during the flick cycle. The flagellum was assumed to be a rigid, tapering curved shaft hinged at the base (but see Fig. 3 for flexural properties during the flick sequence) and of cylindrical cross section (Fig. 5). During a standard downward flick and return the Reynolds number along the flagellum (Re_f) varies according to the curves in Fig. 5B, although only the region of the aesthetasc array (with a leakiness ratio: $z/L_f = 0.5 \rightarrow 1.0$, where z is any point along a flagellum of length L_f) is important for our consideration. In both movements Re_f de-

creases with increasing z/L_f due to a reduction in flagellum diameter and in the normal component of velocity closer to the tip. Using the Flow and Heat Transfer Solver (FAHTSO) code developed by Rosales et al. (2000; 2001) numerical calculations were made to determine the transient, developing 2-dimensional motion of water past a circular cylinder, ultimately attaining a value of $Re_f = 50$ for a downward flick or $Re_f = 30$ for an upward return trajectory. The result of these calculations are shown in Fig. 5C where U_{in}/U_o is dimensionless velocity, t^* is dimensionless time, and x_f/d_f is the dimensionless distance traveled by the approaching flow in units of the flagellum diameter. From these curves and specified boundary conditions the near-field flow streamlines around the flagellum could be calculated and visualized as in Fig. 6. An important dominant characteristic produced within the flow is the development of paired vortices in the wake of the moving flagellum (Fig. 6D). Although of little consequence during the downward flick, developing vortices within the wake of a returning flagellum could be potentially beneficial in delivering odorant-laden water to the aesthetasc array along the ventral flagellar surface. The enhanced fluid motion within the vortex can act to reduce the thickness of the boundary layer surrounding the aesthetascs, allowing for the advective transport of odors to penetrate closer to aesthetasc surfaces. This process effectively decreases the distance over which slower molecular diffusion must occur, enhancing the Péclet number (i.e., the rate of advection of a flow to its rate of diffusion) around the aesthetasc surfaces for odorant delivery. However, the specific role of paired vortices in odorant detection needs to be critically addressed through both experimental and modeling studies. Additionally, because the distal dendrites of the olfactory neurons, with their membrane receptors, reside within the lumen of the aesthetasc, molecular

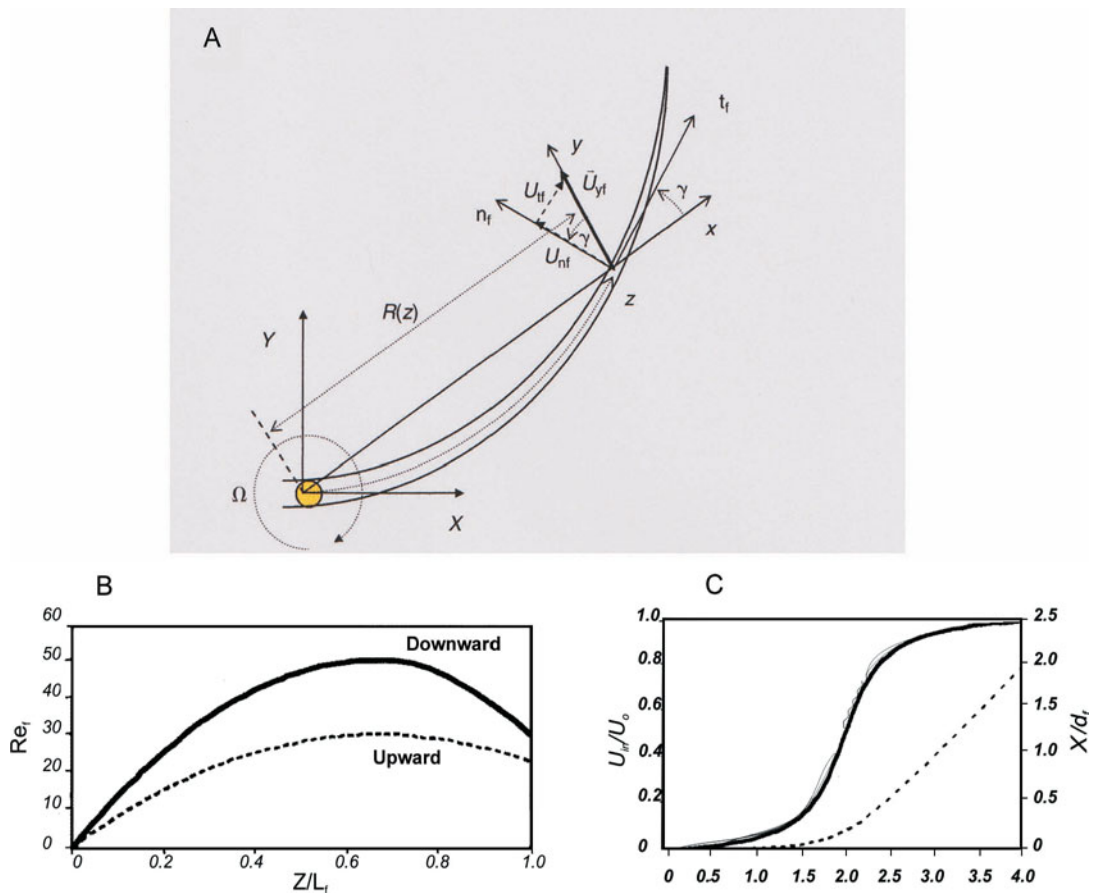
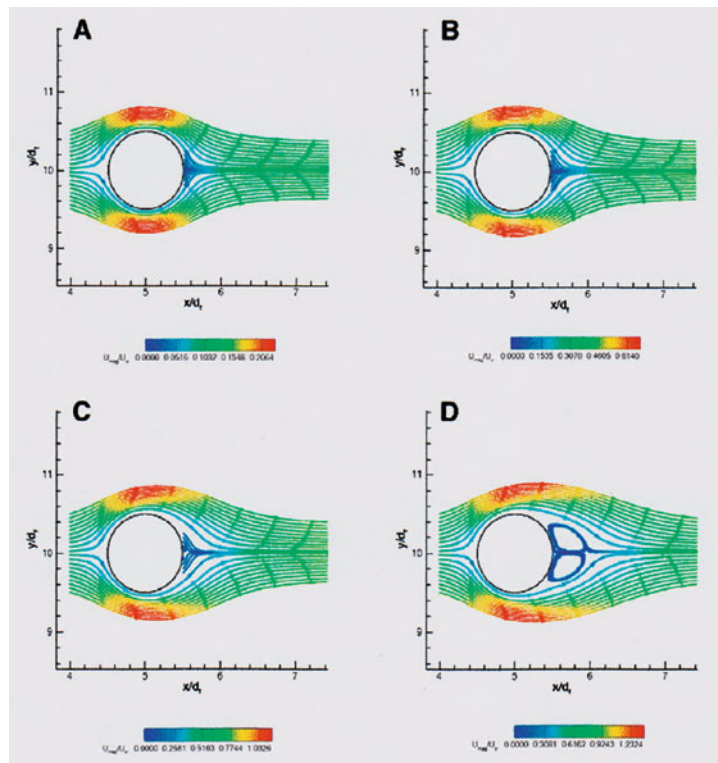


Fig. 5 **A** Schematic model of the crayfish lateral flagellum used in Humphrey and Mellon (2007). The curved, tapering shaft is assumed to be rigid and hinged (yellow circle) at the bottom during a downward flick at angular velocity Ω in relation to the pivot point in a standard X-Y coordinate system. During a flick, the approaching local fluid velocity relative to an x-y coordinate system fixed at point z and normal to the secant $R(z)$ is U_{yf} . The approaching fluid generates components $U_{nf} = U_{yf}\cos\gamma$ and $U_{tf} = U_{yf}\sin\gamma$ normal (n_f) and tangent (t_f) to the flagellum. **B** Variation in Reynolds number Re_f along the dimensionless flagellum during a flick downward ($\Omega = 5.24 \text{ rad s}^{-1}$; heavy line) and during the return stroke (upward, $\Omega = 3.14 \text{ rad s}^{-1}$; dashed line). Decreases in flagellum diameter from base to tip and of the normal component of velocity with increasing nearness to the tip account for reduction in Re_f with increasing z/L_f . **C** Heavy line is the dimensionless velocity, U_{in}/U_o , approximating the acceleration of far-field flow approaching a flicking flagellum as a function of dimensionless time, $t^*(\sim tU_o/d_f)$. The broken line, x_f/d_f , is the dimensionless distance traveled by the approaching flow in units of flagellum diameter. For a standard flagellum, $U_o = 8.63 \times 10^{-2} \text{ ms}^{-1}$ and $d_f = 5 \times 10^{-4} \text{ m}$. Reproduced with permission from Humphrey and Mellon (2007)

diffusion of odorant molecules across the sensillar cuticle must occur for effective odorant capture. While the thickness of the aesthetasc cuticle has been measured in *P. clarkii* as $\sim 1.9 \mu\text{m}$ (Mellon et al. 1989) and in *Panulirus* as $\sim 1.5 \mu\text{m}$ (Grünert and Ache

1988), diffusion coefficients across the aesthetasc cuticle for amino acids, which are major effective olfactory stimuli for aquatic crustaceans, remain unknown factors in this stage of the process. Ultimately, this gap in our knowledge obstructs a complete and

Fig. 6 Near-field flow streamlines with dimensionless velocity magnitude (color) superimposed for the 2D flow accelerating past a flagellum from left to right, according to the far field approaching velocity S-curve plotted in Fig. 5C. Results are shown at times $t^* = 1$ (A $Re_f = 2.6$), $t^* = 2$ (B $Re_f = 25$), $t^* = 3$ (C $Re_f = 47.1$) and $t^* = 4$ (D $Re_f = 50$). Between $t^* = 3$ and $t^* = 4$ the flow separates at the top and bottom of the flagellum to form a recirculating flow region containing two vortices downstream of the flagellum. Reproduced with permission from Humphrey and Mellon (2007)



comprehensive interpretation of the functional significance of antennular flicking in all crustaceans regardless of our understanding of fluid flow around the aesthetascs themselves.

5. Adaptations to terrestrial lifestyle

A number of crustaceans have adopted a secondary, obligatory terrestrial lifestyle but maintain their antennular flicking behavior. Prominent among these are members of the hermit crab family Coenobitidae, tropical crustaceans that are exclusively terrestrial as adults and which possess a highly sensitive olfactory sense (Ghiradella et al. 1968;

Rittschoff and Sutherland 1986). The best known member of this family is the Caribbean land hermit crab, *Coenobita clypeatus*, individuals of which are often sold in pet stores. The largest animals of this family (in fact, the largest land-living invertebrate in the world!) are individuals of the single-species genus *Birgus latro*, native to islands of the South Pacific and Indian Oceans. Except for a brief marine larval period, these animals are entirely terrestrial and live as omnivorous scavenger/predators on remote islands. They have a well-developed sense of smell and can be attracted to suitable baits, which they track employing an antennular flicking behavior reminiscent of marine hermit crabs (Stensmyr et al. 2005). No data are available concerning the velocity of flicking antennular flagella in either *Coenobita* or *Birgus**, but if it is similar to that of *Panu-*

* Bill Hansson (personal communication) suggests that the velocity of an antennular flick in *Birgus* is about 1 cm/sec.

lirus ($0.06 \text{ m}\cdot\text{sec}^{-1}$) then the blunt, peg-like aesthetascs of *Birgus* (dimensions: $100 \mu\text{m}$ long by $40 \mu\text{m}$ in diameter) must operate at Re values only about 10 times smaller than those of *Panulirus*, since the kinematic viscosity of air at 25°C is more than fifteen times that of water ($15.68 \times 10^{-6} \text{ m}^2/\text{sec}$). This means that the aesthetascs of *Birgus* operate within the range where boundary layer shedding could be achieved by antennular flicking, especially if the angular velocity turns out to be 2–3 times higher than that found in the spiny lobster.

The array of aesthetascs on the antennules of both *Coenobita* (Ghiradella et al. 1968) and *Birgus* (Stensmyr et al. 2005) is dense, and in neither case are individual sensilla separated by more than two diameters near the tip. Therefore, questions arise concerning the leakiness of the array to fresh odorant-laden fluid. Among the factors to be considered when attempting to arrive at an answer is the fact that, in contrast to the situation in aquatic environments, air-borne odorants are volatiles and as such, exist in the gaseous phase and have diffusion coefficients roughly 100 times larger than those of dissolved water-borne organic odorants. A second consideration involves the physical design of the coenobitid aesthetascs. Unlike those found on aquatic species of hermit crabs and other crustaceans like crayfish and spiny lobsters (Grünert and Ache 1988; Mellon et al. 1989), the aesthetascs are short and stubby (Fig. 7). Electron micrographic examination of the aesthetascs in *Coenobita* and *Birgus* (Ghiradella et al. 1968; Stensmyr et al. 2005, respectively) reveal them to have an asymmetrical structure: the surface cuticle of that region of the aesthetasc facing the antennule is heavy and thick, while the cuticle facing the environment is thin and crenulated, possibly as a mechanism to increase surface area. Both studies cited above have especially stressed that the short, blunt aesthetascs of *Birgus* and *Coenobita* are

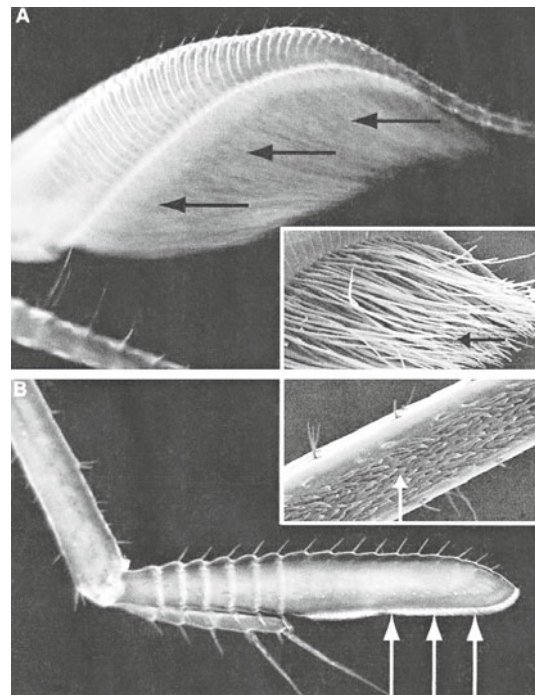


Fig. 7 **A** Distal tip of the antennule in the hermit crab *Pagurus berhardus*, a marine species. The tuft of aesthetascs (black arrows) consists of long, slender sensilla (image courtesy of S. Harzsch from Hansson et al. 2010). Inset is a scanning electron micrograph of the aesthetasc tuft, courtesy of B. Hansson and E. Sjöholm, from Hansson et al. (2010). **B** Aesthetasc array (white arrows) on the distal flagellum of the antennule in *Coenobita clypeatus* (courtesy of S. Harzsch, from Hansson et al. 2010). Inset is a SEM of aesthetascs from *Coenobita*, courtesy of B. Hansson and E. Sjöholm from Hansson et al. (2010)

more similar to chemoreceptive hairs of insects than to the long, slender morphology of marine crustacean aesthetascs. Furthermore, the basal bodies and ciliary segments of coenobitid olfactory dendrites are, like those of insects, surrounded by a lymph space and are housed within the flagellum rather than within the sensilla, as found with aquatic crustaceans (Stensmyr et al. 2005). These differences from aquatic crustaceans suggest convergent evolutionary adaptations that address physical differences (for

example, exposure to dehydration) between the aquatic and terrestrial environments.

Conclusions

Comparative studies on the aesthetasc distribution patterns and size in a variety of different crustaceans are needed to provide a comprehensive picture of the functional significance of antennular flicking behavior to odorant capture. These studies should include experimental observations as well as modeling studies to determine the most appropriate interpretation of the morphology and anatomical distribution of aesthetascs in crustaceans with a variety of lifestyles. Of significant importance are questions about leakiness of sensillar arrays to fluid flow and the role of antennular wake vortices in abetting sensillar access to fluid flow. Adaptations to a terrestrial existence are apparent in some species as well, and these morphological differences require fluid mechanical interpretation, given the differences between the aquatic and the atmospheric environments.

Acknowledgements

The authors wish to thank Dr. J. A. C. Humphrey for helpful discussions and encouragement, Dr. W. O. Friesen for critical help with flicking video imaging, and the National Science Foundation (CBET-0933034) for partial support of the research for this chapter.

References

- Cheer AYL, Koehl MAR (1987a) Paddles and rakes: Fluid flow through bristled appendages of small organisms. *J Theor Biol* 129: 17–39
- Cheer AYL, Koehl MAR (1987b) Fluid flow through filtering appendages of insects. *IMA J Math Appl Med Biol* 4: 185–199
- Finelli C M, Pentcheff ND, Zimmer-Faust RK, Wethey DS (1999) Odor transport in turbulent flows: Constraints on animal vegetation. *Limnol Oceanogr* 44: 1056–1071.
- Ghiradella HT, Case JF, Cronshaw J (1968) Fine structure of the aesthetasc hairs of *Coenobita compressus* Edwards. *J Morph* 124: 361–385
- Goldman JA, Koehl MAR (2001) Fluid dynamic design of lobster olfactory organs: High speed kinematic analysis of antennule flicking by *Panulirus argus*. *Chem Senses* 26: 385–398
- Grasso FW, Basil JA (2002) How lobsters, crayfishes, and crabs locate sources of odor: current perspectives and future directions. *Curr Opin Neurobiol* 12: 721–727
- Grünert U, Ache BW (1988) Ultrastructure of the aesthetasc (olfactory) sensilla of the spiny lobster *Panulirus argus*. *Cell Tissue Res* 251: 95–103
- Hansson BS, Harzsch S, Knaden M, Stensmyr M (2010) The neural and behavioral basis of chemical communication in terrestrial crustaceans. In: Breithaupt T, Thiel M (eds) *Chemical communication in crustaceans*. Springer-Verlag, New York
- Humphrey JAC, Mellon DeF (2007) Analytical and numerical investigation of flow past the lateral antennular flagellum of the crayfish *Procambarus clarkii*. *J Exp Biol* 210: 2969–2978
- Koehl MAR (1995) Fluid flow through hair-bearing appendages: Feeding, smelling and swimming at low and intermediate Reynolds numbers. *Symp Soc Exp Biol* 49: 157–182
- Koehl MAR (2000) Fluid dynamics of animal appendages that capture molecules: arthropod olfactory antennae. In: Fauci L, Gueron S (eds) *Computational modeling in biological fluid dynamics*. IMA volumes in Mathematics and its Applications, Vol 124. Springer-Verlag, New York, pp97–116
- Koehl MAR, Koseff JR, Crimaldi JP, McCay MG, Cooper T, Wiley MB, Moore PA (2001) Lobster sniffing: Antennule design and hydrodynamic filtering of information in an odor plume. *Science* 294: 1948–1951
- Louden C, Best BA, Koehl MAR (1994) When does motion relative to neighboring surfaces alter the flow through arrays of hairs? *J Exp Biol* 193: 233–254
- Mellon DeF (1997) Physiological characterization of antennular flicking reflexes in the crayfish. *J Comp Physiol A* 180: 553–565
- Mellon DeF, Tuten HR, Redick J (1989) Distribution of radioactive leucine following uptake by olfactory sensory neurons in normal and heteromorphic crayfish antennules. *J Comp Neurol* 280: 645–662
- Mellon DeF, Humphrey JAC (2007) Directional asymmetry in responses of local interneurons in the crayfish deutocerebrum to hydrodynamic stimulation of the lateral antennular flagellum. *J Exp Biol* 210: 2961–2968

- Reidenbach MA, George N, Koehl MAR (2008) Antennule morphology and flicking kinematics facilitate odor sampling by the spiny lobster, *Panulirus argus*. *J Exp Biol* 211: 2849–2858
- Rittschoff D, Sutherland JP (1986) Field studies on chemically mediated behavior in land hermit crabs (*Coenobita rugosus*): Volatile and non-volatile odors. *J Chem Ecol* 12: 1273–1284
- Rosales JL, Ortega A, Humphrey JAC (2000) A numerical investigation of the convective heat transfer in unsteady laminar flow past a single and tandem pair of square cylinders in a channel. *Num Heat Transfer A* 38: 443–465
- Rosales JL, Ortega A, Humphrey JAC (2001) A numerical simulation of the convective heat transfer in confined channel flow past square cylinders: comparisons of inline and offset tandem pairs. *Int J Heat Mass Transfer* 44: 587–603
- Snow PJ (1973) The antennular activities of the hermit crab, *Pagurus alaskensis* (Benedict) *J Exp Biol* 58: 745–765
- Stacey MT, Mead KS, Koehl MAR (2002) Molecule capture by olfactory antennules: Mantis shrimp. *J Math Biol* 44: 1–30
- Stensmyr MC, Erland S, Hallberg E, Wallén R, Greenaway P, Hansson BS (2005) Insect-like olfactory adaptations in the terrestrial giant robber crab. *Curr Biol* 15: 116–121
- Tierney A-J, Thompson CS, Dunham DW (1986) Fine structure of aesthetasc chemoreceptors in the crayfish *Orconectes propinquus*. *J Can Zool* 64: 392–399
- Webster DR, Weissburg MJ (2001) Chemosensory guidance cues in a turbulent chemical odor plume. *Limnol Oceanogr* 46: 1034–1047